Optical spectroscopy of impurity atoms in semiconducting Nanowires

Shishir Shroff

Master's Thesis
2017

LUND
UNIVERSITY

Division of Solid State Physics
Department of Physics
Lund University

Master's thesis which, by due permission of the Faculty of Engineering at Lund University, Sweden, will be publicly defended on Wednesday, January 18, 2017 for the degree of Master's in Physics.

Dan Hessman
Supervisor

Joakim Cederkall
Faculty opponent

Lund University

Contents

Abstract

In a small and confined one dimensional geometry of nanowire, even few defects can influence the performance of the devices. Main objective of this thesis is to conduct photoluminescence study of such defect states in GaAs nanowires, which we will first introduce by diffusing copper impurity atoms, in very low concentrations.

In low concentrations, ideally single atom in a wire, the photoluminescence outcomes is expected to be influenced by the position of copper impurities in the wire. Therefore, these defect states can act as local probes in the material and provide useful information about the recombination kinetics. Single defects can be used to understand the effect of dielectric screening on the ionization energies of the impurities, within a nanowire.

As a part of this thesis, PL studies of high quality GaAs nanowires, which demonstrated benchmark solar cell performance, were conducted. Experiments were conducted to identify the conditions for diffusing copper in GaAs at low temperatures. As a part of this thesis, a dedicated PL setup, optimized for defect studies was assembled and a positioning scheme was developed to perform PL measurements on same nanowires before and after the diffusion.

Band gap luminescence peak for as grown GaAs nanowires was found ~10meV red shifted from theoretical values, and an attempt has been made to provide reason out the same. By comparing luminescence peak, before and after diffusion, associated with copper acceptor states in GaAs, it was confirmed that copper diffusion was successfully achieved at lower temperatures of 450^{o}C. But, the possibility of creating single defect states was limited by background contamination of copper in our samples.

Abbreviations

1D	one-dimensional
Au	gold
Cu	copper
CB	conduction band
CCD	charge-coupled device
EDX	energy-dispersive X-ray spectroscopy
E_g	band gap
GaAs	gallium arsenide
GaP	gallium phosphide
GOR	giant oscillation strength
In	indium
MOVPE	metalorganic vapor phase epitaxy
NP	nanoparticle
NW	nanowire
PL	photoluminescence
SEM	scanning electron microscopy
TEM	transmission electron microscopy
VB	valence band
VLS	vapor-liquid-solid
WZ	wurtzite
XRD	X-ray dispersive spectroscopy
ZB	zincblende

1 Introduction

A piece of semiconductor is the functional unit in all our electronic products. What makes it useful is the separation of the conduction and valence electron states by a forbidden energy gap. This imparts a nonlinear conducting behavior , which can be tuned for specific applications and exploited for controlling the conduction of electrons at will. Group IV elements, which lie in the middle of the periodic table, show semiconducting properties. Binary and ternary combinations of Group II and Group VI, Group III and Group V are also semiconducting and used in different applications.

While Si, a group IV semiconducting element, dominated semiconductor research in the early decades, a compelling need for better performing devices has fueled research in the direction of III-V novel materials and structures. Constant miniaturization has pushed the sizes to nanometric dimensions, creating new fundamental possibilities as well as challenges. Semiconductors can now be crystallized in the form of nano spheres, cubes, pyramids etc. A semiconducting nanowire is a rod like structure ~100nm or less in diameter and a few micrometers long. Sophisticated techniques are required to grow and characterize them. Methods like scanning electron microscopy, tunneling electron microscopy and x-ray diffraction can physically determine the shape, size, morphology, structure and composition of the nanowire.

The energy band structure in a semiconductor, which determines the electrical properties, is sensitive to imperfections in the lattice structure of the material and defect states created by impurity atoms. The effect is highly pronounced for a confined 1 D structure like nanowires, due to charge confinement, coulomb repulsion etc. Photoluminescence (PL) spectroscopy is a sensitive tool which can be used to correlate this effect. In fact specific defects can be artificially created in the system to conduct a controlled study using photoluminescence.

Nanowire devices have shown tremendous progress in solar cells and LED applications. Further improvement in performance of these devices is limited, to a large extent, by the occurrence of defects, limitations in the synthesis process to remove them, and the complications involved in studying them [1] [2]. With better understanding and control of its

synthesis process, the quality of the nanowires has improved significantly in the last decade. This has opened an opportunity to conduct fundamental studies of these structures. Although much needed, not enough work has been done in this direction so far.

This thesis aims to conduct a photoluminescence study of artificially created individual deep defect states in semiconductor nanowires. We intend to create such defect states by diffusing copper atoms in GaAs. Deep defect states are related to the ionization energies of the material and less related to the band edges. These defects can therefore act as local probes to understand for instance, the band offset in the 2 metastable states of GaAs in nanowires, ZB and WZ which is still disputable. In addition, individual defect studies can also help us relate charge confinement and surface phenomenon to the kinetics of electron hole pair recombination.

2 Theory

Bandgap study using Photoluminescence Spectroscopy

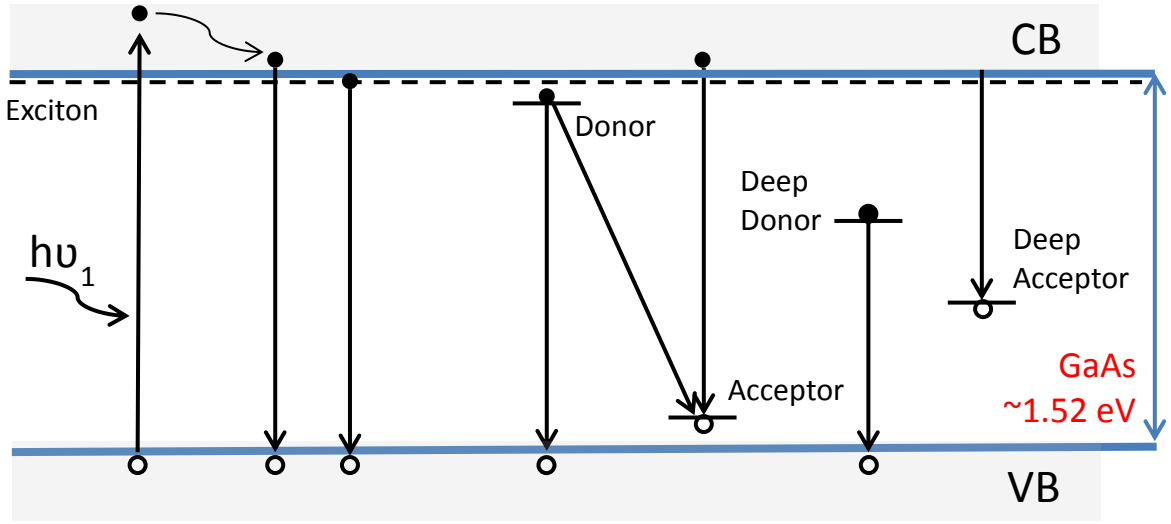

Figure 2.1: *Schematic of a PL excitation and recombination mechanism.*

Photoluminescence spectroscopy can be used to study the band gap or defects related energy states of a semiconductor. The principle of this process is schematically represented in figure 1. In a semiconductor, conduction and valence states of electrons are separated by an energy gap, where electrons are forbidden. At lowest temperatures, all the electrons occupy the valence band and the conduction band is empty. A valence electron can be excited to the conduction band if it absorbs a photon of energy more than or equivalent to the band gap (E_g). The excited electron leaves behind a hole in the valence band creating a free electron hole pair in the process. The electron hole pair can recombine either radiatively by releasing a photon, or non-radiatively. In the photoluminescence technique the emitted photons are collected and the distribution of the energy of the photons is used to understand the band gap and other defects states in semiconductor. Radiative recombination occurs primarily by three different mechanisms.

In the first case, the electron in the conduction band combines with a hole in the valence band. The photon emitted has an energy which is equivalent to the band gap of the semiconductor. In the second case, an electron bound to a donor impurity recombines with a hole in the valence band or an electron in the conduction band recombines with a hole bound to an acceptor impurity. The energy of the photon released in this process is less than

the band gap, by a value equivalent to the binding energy of the impurity atoms. The third case is the excitonic transition, which occurs due to the recombination of an exciton. In the next section, the physics of excitons will be further discussed.

2.1 Excitons

An exciton is a neutral quasi-particle, created when a free electron and hole are bound in a paired state, due to Coulombic interaction, reducing its energy to less than the band gap energy by a value equal to the binding energy of the exciton. This energy difference appears as a shift of the luminescence peaks from the bandgap energy. Excitonic transitions are very strong for low temperatures (~2-10k) and quench rapidly with an increase in temperature [7]. They are referred to as signature transitions of a particular semiconductor in a low temperature PL spectrum, which highlights their importance.

Excitons in semiconductors are described by the Wannier equation and are called Wannier-Mott excitons. The wave function of such an exciton is strongly delocalized and they are free to move inside the crystal, therefore they are also termed as free excitons. A free exciton can be approximated with a Bohr model of hydrogen, where the electron and hole revolve around each other bound by an attractive force, given by equation 2.1,

$$U(r) = -\frac{e^2}{4\pi\varepsilon\varepsilon_o r} \tag{2.1}$$

where

e is the electron charge,

r is the electron hole distance,

ε_o is the permittivity of the vacuum and

$\mathcal{E}$ is the relative permitivity of the material.

However, the binding energy for a free exciton is much less and the radius is much larger than for the hydrogen atom. This is due to the low effective masses of electrons and holes in a semiconductor, as opposed to the electron and proton in the hydrogen atom, and screening effects due to dielectric of the host semiconductor. The free exciton radius and energy can be calculated using equation 2.2 and 2.3

Free exciton radius, $r_n = -\frac{\varepsilon}{m_r/m_o} n^2 \alpha_B$ (2.2)

Energy of the free exciton, $E_{x(n)} = -\frac{m_r/m_o}{\varepsilon^2} \frac{1}{n^2} R_y(H) = \frac{E_x}{n^2}$ (2.3)

where

α_B ~$5\text{x}10^{-2}$nm is the Bohr radius of the hydrogen atom,

n is the principal quantum number of the orbit,

R_y(H) =13.6eV is the binding energy of the ground state of the hydrogen atom.

For GaAs, the free exciton energy is calculated as ~4.9 meV. This energy is very small and comparable to the thermal energy, k_BT at 50 K. At higher temperatures, exciton can easily breakup by colliding with phonons. Therefore, it can be said that the excitons are weakly bound and can only occur at low temperatures.

2.2 Bound excitons

Various defects in the semiconductor make effective trapping sites for the free excitons. Due to their mutual interaction, free excitons can effectively get bound to these defect states by losing their kinetic energy. Bound states are more localized and their radiative recombination emits a photon with less energy, as compared to the free exciton. The actual value of this energy depends on the impurity or defect state that binds the exciton.

The free excitons can bind to neutral shallow impurities, charged shallow impurities or isoelectronic impurities, creating different features in the PL spectra. Complex excitonic species like bound multi-exciton complex or self-trapped exciton complexes can also exist in certain materials. But for GaAs, donor or acceptor bound excitons are more relevant and therefore this discussion is limited to that. [3] For direct band gap materials like GaAs, the efficiency of luminescence from bound excitons is observed to be higher than the free exciton emissions. This is explained by the high trapping probablility and the so called giant oscillator strength, which is discussed hereafter.

τ_{tr}, the free exciton lifetime before it is trapped**,** defines the trapping probability of a free exciton to a bound state. τ_{tr} is of the order of ~10^{-9}s and can be calculated using equation 2.4,

$$\tau_{tr} = \frac{1}{\sigma_x N v} \quad (2.4)$$

Where,

v is the thermal velocity of exciton diffusion, typically 10^6 cm/s at 2 K,
$\sigma_x \approx \pi a_x^2$, is the capture cross section, $\approx 10^{-12}$ cm^2 for Bohr radius $a_x \approx 5$ nm at 2 K,
N is the defect concentration, ~10^{15}/ cm^3 (nominal value in a III-V semiconductor),

The free exciton lifetime, $\tau_{tr,}$ is experimentally found using time resolved measurements to be ~1.9 ns in GaAs, which is comparable to the radiative recombination lifetime τ_r of the free excitons. [4] Therefore there is an equal probability for a free exciton to be trapped in a bound state or recombine radiatively.

Oscillator strength is the probability of emissions of photons in the transition between different energy states. Oscillator strength in brief implies that inside an exciton volume of a_x^3, around the impurity atom or defect, all the unit cells contribute to the radiative recombination of the bound exciton. [5] This is due to the coherent polarization of the lattice, which is pronounced for materials like GaAs, which have small exciton binding energy. For impurity bound excitons, a higher oscillator strength imparts them shorter radiation lifetimes. This increases the probability of radiative recombination and makes it more luminescence efficient as compared to the free exciton. Further discussion is beyond the scope of this work.

2.3 Photoluminescence studies of bulk GaAs

GaAs is a large direct band gap semiconductor material with E_g = 1.52 eV which emits luminescence in the near infrared region. Using PL spectroscopy the radiative transition mechanisms in the bulk ZB GaAs wafers have been extensively studied. The energy band gap of GaAs at T≤21K was established to be 1.521 eV, by findings of Sturge et al [15]. Calculations done by Sharma and Rodriguez conclude the possibility of both ionized donor and acceptor bound excitons in the same material. Using these results the binding energies of free and bound excitons can be calculated[7][8].

In a PL spectrum of GaAs the bound exciton states are associated with emission of photons with energy

$h\upsilon_{(D^0X)} = E_G - E_D{}^0{}_X = 1.515$ eV

$h\upsilon_{(D^+X)} = E_G - E_D{}^+{}_X = 1.5133$ eV

$h\upsilon_{(A^0X)} = E_G - E_A{}^0{}_X = 1.491$ eV

$h\upsilon_{(A^-X)} = E_G - E_A{}^-{}_X = 1.481$ eV

Experimentally determined values show deviation from these values because of approximations in the theoretical model and different experimental conditions.

2.4 Defects in GaAs NWs

GaAs has a high electron and hole mobility which means that the charge carriers can easily find a defect state, usually lower than the band gap, which then becomes a favorable recombination center. Therefore, it should be possible to detect even trace amounts of defect states.

First of all, GaAs has a high surface recombination velocity (~10^5 cm/s) and due to an increased surface to volume ratio of the NWs, the surface phenomena dominate the intrinsic recombination mechanism in the GaAs NWs[9]. PL efficiency is highly reduced due to the various surface oxides and charge states, which act as non-radiative recombination centers. A lattice matched AlGaAs shell is therefore often grown to passivate the surface mediated Shockley-Read-Hall recombination, increasing the PL efficiency. Also, some other techniques e.g. modulation doping are used to achieve similar results. This can further create additional interface states and impurity states.

Secondly, GaAs, which is Zinc blende (ZB) in bulk phase is found to be metastable in Wurtzite (WZ) phase as well when grown in a nanowire geometry. Both ZB and WZ GaAs have same band gap but WZ GaAs exhibits a certain band offset from the ZB structure. Due to which a ZB-WZ interface shows a type II recombination in a PL spectrum. Since the composition of both ZB and WZ GaAs is the same, intermixing of these phases creates inhomogeneity within the nanowire which can result in additional effects on PL spectra.

In the past few years, the quality of nanowires has improved significantly. This has now made it possible to conduct detailed luminescence studies of nanowires. In GaAs NWs, ZB and WZ interfaces have been artificially grown to study the type II transitions between them [10]. Also there is continuous work going on to incorporate impurities by in-situ doping during growth. For various NWs, in-situ incorporation of zinc, carbon, selenium, sulphur etc in III-V NWs have been successfully reported. For GaAs NWs, in-situ doping options are possible but scarce and there are scaling limitations as well.

Prior to this thesis, some attempts were made to ion-implant Mn in GaAs NWs. The attempts were not successful because the NWs stopped luminescing after implantation. This was due to lattice defects created in the nanowire when bombarded with high energy atoms. Less ionic materials like GaAs can be easily amorphized by ion implantation, severely degrading the PL efficiency.

Introducing impurities in NWs by diffusion has not been reported anywhere, to the best of my knowledge. Elevated temperatures, more than 800^{o}C, are required to diffuse high concentration of impurities in GaAs. GaAs NWs are typically grown at 500-600^{o}C and they are not stable for temperatures higher than this. This has discouraged further research in this direction. But it should be possible to diffuse impurities, in low concentrations, at much lower temperature, without degrading the NW. This would be perfect for individual defect studies and was the starting point for this thesis.

3 Experimental procedure and setup

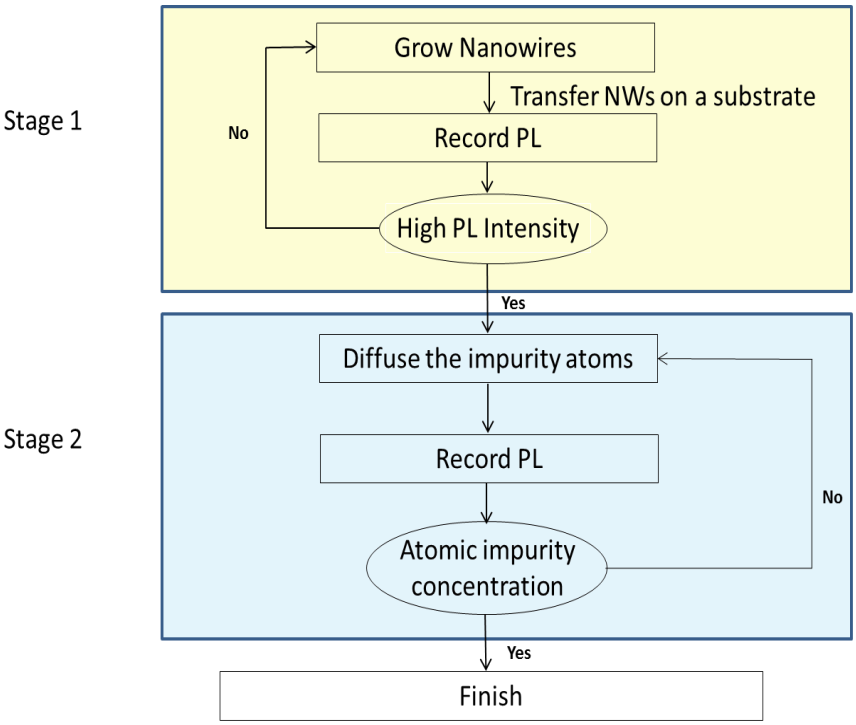

Figure 3.1: *Proposed experimental work flow of this thesis.*

Figure 3.1 shows the experimental work flow for this thesis. Since no standard recipe or previous work was available, the project involved many iterative steps. NWs for this thesis were provided to us. We started with PL study of the as-grown NWs, to identify a NW sample suitable for this study. The selected NWs were diffused with copper, under different conditions, until the PL study could confirm the presence of copper in the NWs. Only after establishing the diffusion parameters, attempts could be made to reduce the impurity concentration to few atoms in the wire.

Within the purview of this project, different apparatus were assembled and optimized to ensure consistency of the experimental results, avoid errors and extract better performance.

3.1 Photoluminescence studies

In order to detect weak signals from defect states in the NWs, a PL setup was assembled. All possible efforts were made to improve the collection efficiency of the setup and have a higher sensitivity. This would enable us to detect the defect states without using a very high excitation intensity.

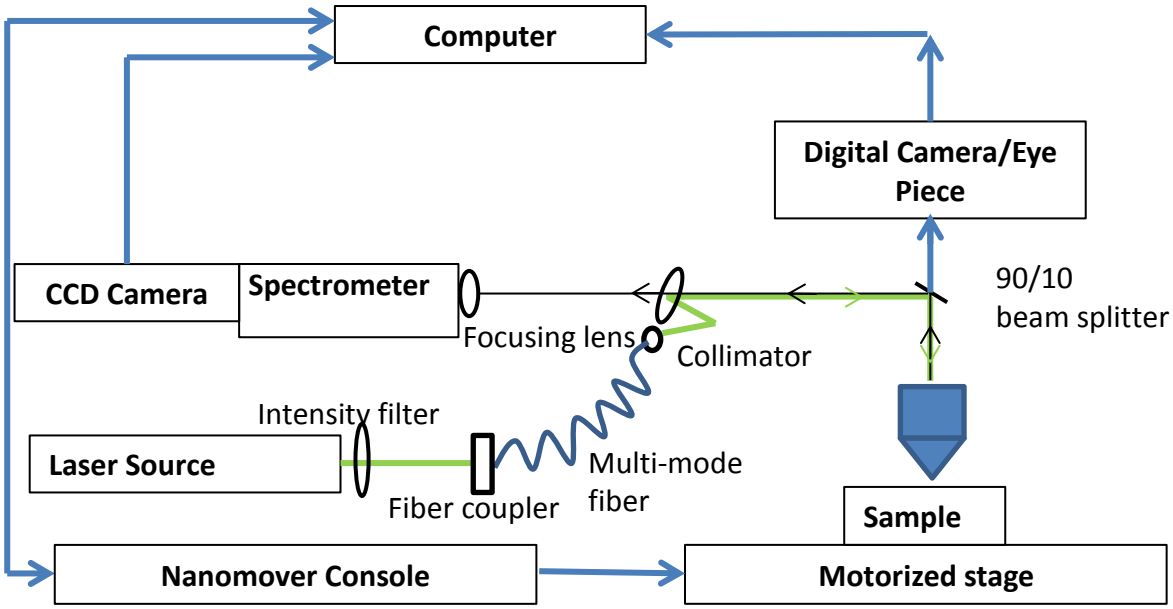

Figure 2.2: *Schematic of the PL setup used for most part of this thesis*

Figure 3.2 shows the schematic of setup, in which a 532 nm Nd:YAG laser was used to excite the sample. A filter wheel with different optical density filters is used to systematically adjust the excitation intensity. Laser coupled to multimode optical fiber is used to illuminate a small spot on the sample, through the objective, in a confocal configuration. The luminescence from the nanowire is collected by a 20x objective and reflected on the spectrometer using a 90-10 beam splitter in the microscope column, which means 90% of the light is reflected towards spectrometer and only 10% passes through and reaches the eye piece. To avoid chromatic aberrations, a commercial DSLR camera objective is used to focus the luminescence signal on the slit. The scattered laser is filtered from the PL signal using a high pass filter before it reaches the objective.

Inside the spectrometer, using a blazed diffraction grating, photons corresponding to different wavelengths are spatially distributed. These photons are then collected by different pixels of a CCD chip to create a luminescence spectrum. Diffraction gratings are characterized by the density of the grooves, which determines how well it can resolve different wavelengths. Higher grooves per grating can resolve the wavelengths more efficiently but reduces the spectral range and photon counts for every pixel. A 600 grooves per mm grating was optimally selected, after trying different grating options. The grating dispersion was calibrated using the standard emission lines from a neon lamp, to correct any error in the peak positions of the spectra.

A LN_2 cooled back illuminated silicon chip CCD was used to collect the signal. To minimize the dark noise, CCD is cooled to 140K by using liquid nitrogen. By illuminating the chip from the back, 85% quantum efficiency (QE) at its peak value can be achieved, as compared to the 50% for a standard CCD. However, working in this arrangement, the CCD chip exhibits an interference pattern created by the wavelength of the incident light comparable to the thickness of the chip. This is called etaloning. It was compensated for in our measurements to avoid artifacts. Figure 3.3a shows the dark and bright stripes on the chip when uniformly illuminated with a white light source. These are intereference patterns created due to etaloning effect in the CCD. Figure 3.3b compares the luminescence spectrum of GaAs at room temperature before and after etalon correction. The spectrum before etaloning correction shows fine features on the high energy falling edge of the curve, which clearly become smooth after suitable correction.

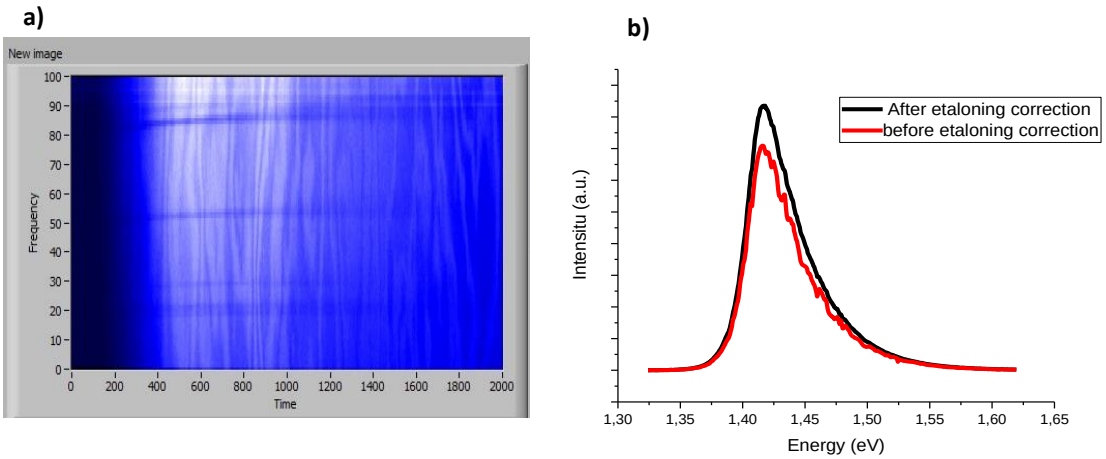

Figure 3.3: ***a)*** *Interference pattern in the CCD due to etaloning effect.* ***b)*** *PL measurement spectrum of GaAs at room temperature before and after etalon correction*

To compare the effects of diffusion experiment on the individual nanowire, it is important to obtain the photoluminescence spectrum of the same nanowire before and after annealing. For measurements on the same single nanowires, a gold patterned substrate is typically used. However, the possibility to use a patterned wafer was ruled out in our case to avoid any contamination while diffusion.

A motorized stage is added to the microscope which can position the nanowires with the precision of 10 nm, endowed by the micro step of the motors. We used the motorized stage to create a method for measuring the same nanowires before and after diffusion, without

the patterned substrate. To implement this, an individual nanowire was located on the substrate, by visual inspection using a microscope, and placed under the laser illuminated small spot. The stage coordinates for the nanowire at this position was saved. This was repeated for 3-4 different nanowires with a PL study conducted before and after diffusion. Additionally two easily identifiable reference features were created on the substrate, by scratching it at two opposite corners. Coordinates for these reference features were also recorded by placing them in the same fixed spot, under the laser. This provided us with a mapping of the nanowires, whose PL spectrum had been recorded before diffusion, with respect to two fixed reference spots on the substrate. The images of the nanowires and reference features were also captured using a digital camera, mounted on the microscope.

After diffusion, the easily identifiable reference features were located, using the saved digital camera images, and placed at the same fixed position, under the laser illumination. New stage coordinates for the reference features were recorded; and a coordinate transformation matrix was calculated by finding the linear and angular shift in the new coordinates of the reference spots. Using the coordinate transformation matrix, the new coordinates of the previously measured nanowires were calculated, and the stage was moved to those positions to find the nanowires. To compensate for errors in the positioning, the images of the nanowires captured before diffusion, were used to identify the nanowire and fine-tuned manually to position it under the laser illuminated spot.

This method was implemented with certain fixed conditions, in which the wafer was roughly placed in the same orientation before and after diffusion/annealing experiment. In the given conditions, the method was fairly reproducible and could be used to consistently locate the nanowires after diffusion, for post diffusion studies. Figure 3.4a and 3.4b gives the 2 images of the same spot in the sample, captured before and after diffusion. The images after diffusion shows some contamination but the nanowire of interest can be distinguished by comparing the overall image.

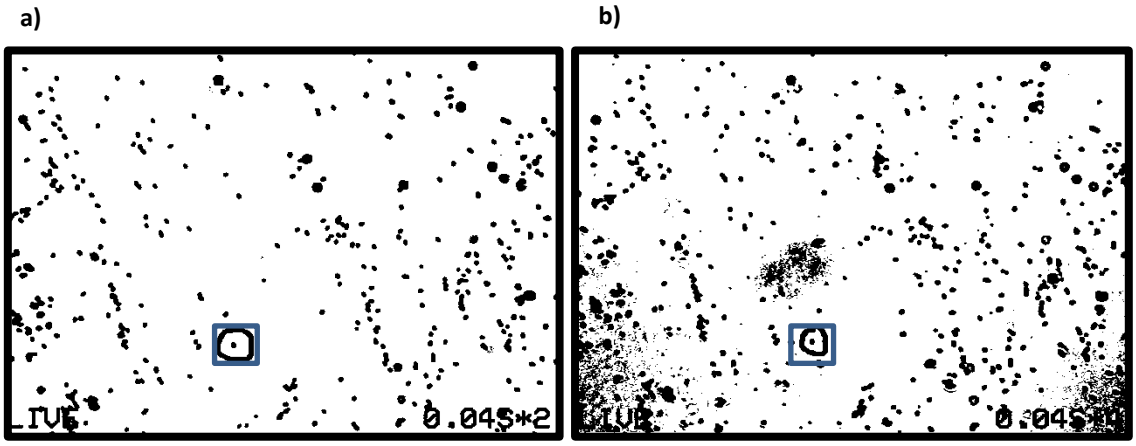

Figure 3.4: a) *Image captured before diffusion shows the nanowire which will be measured* ***b)*** *image captured after the diffusion shows the same nanowire and some contamination around it as well. Both the images are converted to black and white, from original for better contrast.*

For PL measurements, nanowires were broken off from the growth substrate and transferred, at a suitable concentration, onto a non-luminescing Si substrate. The Si substrate with the nanowires was placed on a cryostat cold finger and liquid helium was used to cool down the nanowires to ~4K. For each NW, a series of PL spectra were obtained while varying the laser power.

3.2 Diffusion

To carry out diffusion, the silicon wafer containing nanowire is annealed in a sealed and evacuated quartz ampoule to avoid unwanted contamination, oxidation and out-gasing of As from the nanowires. The sample is first placed in a quartz tube whose one end is already closed. The other end is connected to a vacuum pump, the tube is evacuated to a fixed pressure (10^{-2}mbar) and then the second end is also sealed. A hydrogen gas torch is used to melt and fuse the open end of the tube. The ampoule is then placed in the diffusion furnace preheated to a fixed temperature, generally 350-550^{o}C in this thesis work. The ampoule was removed from the furnace after the desired duration and immediately quenched by rinsing with DI water. Using an electric saw the ampoule was cut open and the sample was retrieved.

In the first diffusion experiment it was noticed that after the sample was removed from the ampoule, it was completely covered with fine particles, shown in figure 3.5. The particles were indistinguishable from the nanowires under the microscope and this made it

impossible to do any post diffusion PL analysis of our nanowires. EDX measurement of the contaminants revealed they are SiO_2 particles, which may come from the fused silica tube used to make ampoules. But it was not sure how these contaminants were deposited on the substrate and in which stage of processing they were incorporated.

Initially it was assumed that the contamination comes from the walls of the ampoule and deposited on the sample while annealing. Therefore, different procedures for cleaning the tube, prior to diffusion were tried. Ultrasonic cleaning of the ampoules in the acetone and IPA did not solve the problem. After this a rigorous cleaning of quartz tube in aqua regia followed by overnight baking of the ampoules at 550^{o}C was tried. Finally, HF etching of the tube was performed, followed by rinsing with DI water and overnight drying at 200^{o}C in an oven. Unfortunately, the problem still persisted.

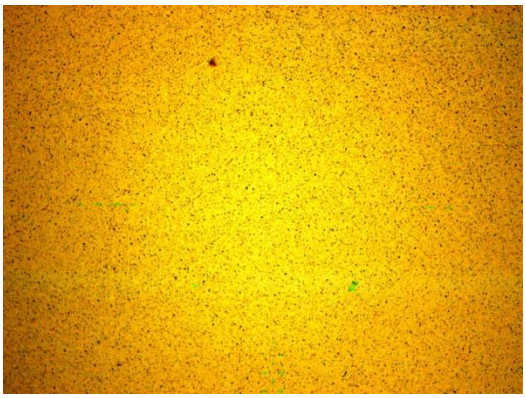

Figure 3.5: *Optical microscope image of the substrate after diffusion.*

It was later found that the particles are actually coming from the silica dust generated and deposited when the ampoule is cut. It was assumed that while cutting, when the ampoule is punctured, the air gushes in due to a low pressure inside the tube. This gust of air carries with it the silica dust which is generated while cutting the ampoule. At this point, a simple and inexpensive alternative to cut the ampoule without generating the silica dust was not found. Instead different attempts were made to avoid the dust from getting deposited on the substrate. Initially different lengths of ampoule were tried, but that had little effect.

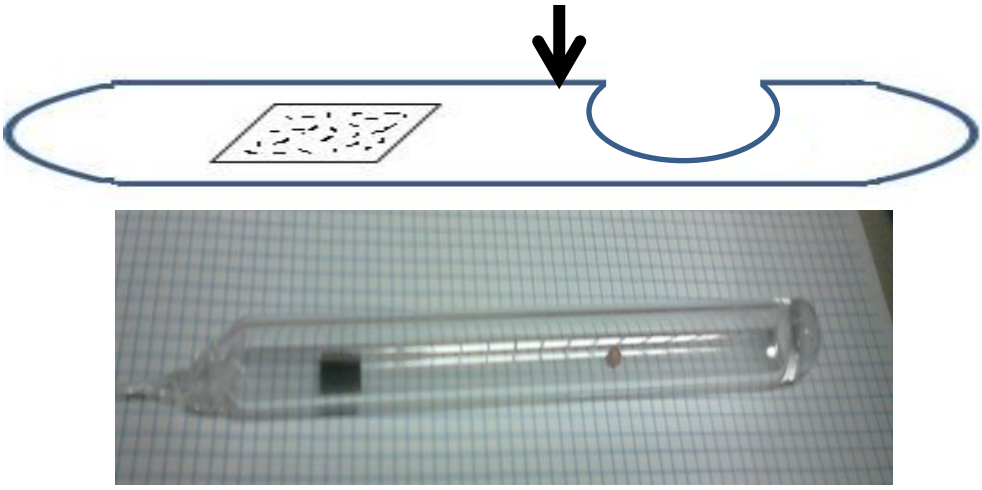

Figure 3.6: a) *Schematic and b***)** *Image of an ampoule with a sample and a notch.*

Finally the problem was solved by creating a small notch by heating the tube at one end, before it is sealed. The ampoule was then cut at a point close to the notch as shown by the arrow in the figure 3.6a, using an electric saw. Water was added drop by drop to the point where the cut is being made. Although it did not ensure an absolutely contamination free surface, the contamination was reduced considerably. The nanowires were distinguishable and post annealing PL measurements could be made. It is not very certain, but the possible explanation is that the notch creates a preferential flow of the dust, mixed with water and air in the direction of the notch. The dust is subsequently deposited on the walls of the tube around the notch and the sample is relatively dust free. This method has been implemented in further experiments with a 80 % success rate.

4 Results and Discussion

Figure 4.1 shows the proposed flow of work for this thesis. To begin with it was important to have a suitable material, which ideally would be a pure semiconductor nanowire that shows only band gap transition peak in the PL spectrum and contains no background impurity or defects. Then the next task was to artificially introduce defect states in atomic concentrations. We proposed to use a heterostructure nanowire as shown in figure 4.1, as the starting material. It shows a GaAs segment grown in a wide band gap material, passivated with a shell.

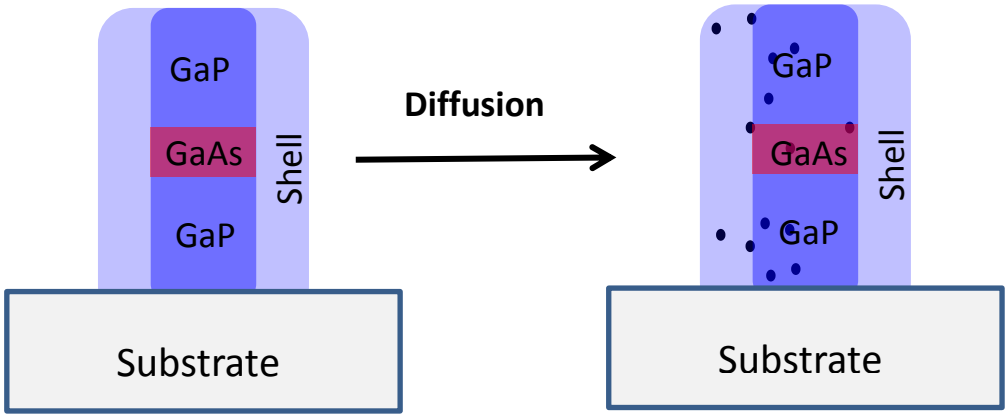

Figure 4.1: *Schematic of the proposed heterostructure nanowire shows GaAs segment in a GaP nanowire with a passivating shell around. The black dots represents arbitrary distribution of the impurity atoms introduced after diffusion.*

It was conjectured that a small GaAs segment would restrict the amount of impurity atoms introduced in it, and distribute most of the defects in the GaP nanowire, as illustrated in figure 4.1. In the PL study defect states introduced in the GaAs would be clearly distinguishable from the defects in GaP, due to different luminescence energy in GaAs and GaP. For a different project at Nanolund, an axial and radial hetrostructure similar to our proposed structure was already being grown for LED applications[1]. This naturally became the starting point of our study. The evaluation of this material is described in section 4.1. After various attempts we concluded that these wires could not be used within the time frame of my project. Therefore, we moved on to high quality nanowires samples, which had shown benchmarking performance in nanowire solar cells. While conducting PL studies of the reference nanowires, a weak luminescence due to copper contamination in our wires was detected. Since we could not have reduced the artificially introduced defect

concentration below the background impurity level, we made a slight deviation from our plan of individual defect studies. We pursued instead a PL study of the individual high quality nanowires. Also for future implementation of this idea, we carried on with our diffusion experiments, to find the optimum conditions for diffusing copper. The results for each of these different experiments are discussed in the next section.

For intensity dependant measurements, the intensity was systematically decreased using optical density filter. The maximum laser intensity was set to P_o= 5 mW and reduction by a factor x resulted in power $10^{-x} P_o$.

4.1 PL results from GaP-GaAs-GaP nanowires

Figure 4.2 shows the PL spectrum from all the hetrostructure nanowire samples grown for this thesis. Initially a series of 4 samples 10394, 10395, 10396 and 10397 were grown, see Appendix A for details. The samples overall exhibited a low PL efficiency, with broad luminescence. Any peak corresponding to the GaAs band gap transition could also not be distinguished. These samples were clearly not suitable for this work since PL signal for artificially diffused defect states would merge with the broad luminescence and would not be detected. Poor surface passivation was proposed to be the possible reason for such a broad luminescence. Therefore, another series of 5 samples 10450, 10451, 10452, 10453, 10454 were grown with different shell thicknesses and different material (Appendix A) to find the optimum recipe.

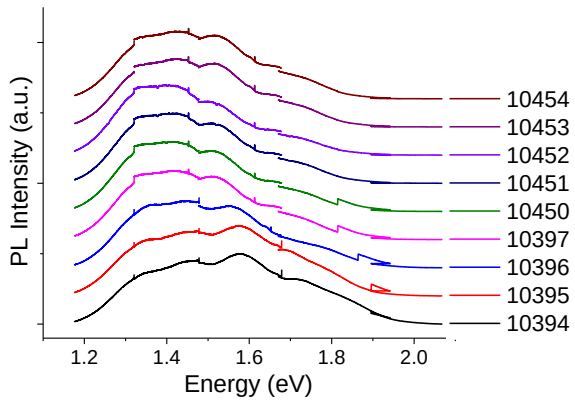

Figure 4.2: *PL spectrum of nanowires from different hetrostructure nanowire samples.*

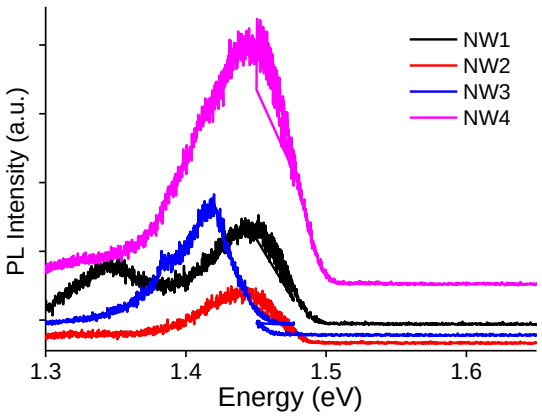

Figure 4.3: *PL spectrum of different single nanowires in sample 10451.*

By comparing the different NWs measured from each sample, sample 10451 seemed to show best results, probably due to a better surface passivation by a thicker AlGaAs shell. Figure 4.3 shows the PL spectrum from 4 individual NWs of sample 10451. It can be clearly seen that the PL results did not show a consistent behavior. This made it challenging for us to analyze these NWs. Three spectra show luminescence peak centered at 1.445 eV. For one of the nanowires, luminescence is observed at 1.42 eV. These peaks may come from a luminescing defect state, situated either in the GaAs segment or the GaP segment. A clear band gap transition peak for GaAs is missing in the spectra and no evident change In the PL spectrum was observed due to the different growth times for the GaAs segment in the core. Due to poor luminescence efficiency and absence of the GaAs band gap associated peaks in the luminescence no further conclusions could be drawn at this stage.

Since NW growth was not a part of this project and a heterostructure with many interfaces would require a lot of time to optimize, further investigations of these nanowires were abandoned at this stage.

4.2 PL results from GaAs-AlGaAs core shell nanowires

After initial failures to grow the heterostructure NWs, the high quality core shell GaAs/AlGaAs NWs showing a record 15.3% solar cell efficiency were investigated [11]. The NWs in the preliminary PL measurements exhibited a strong luminescence close to the band gap energy in GaAs. Prior to diffusion experiments, intensity dependent PL measurement of many different NWs were conducted, which revealed certain interesting results. The observations are discussed in detail in the following sections.

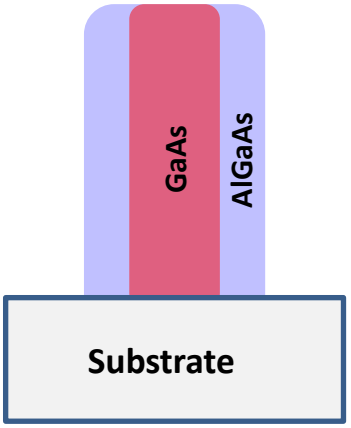

Figure 4.4 *Schematic of the core-shell GaAs nanowire used for the PL studies.*

4.2.1 Probing the background impurity signal

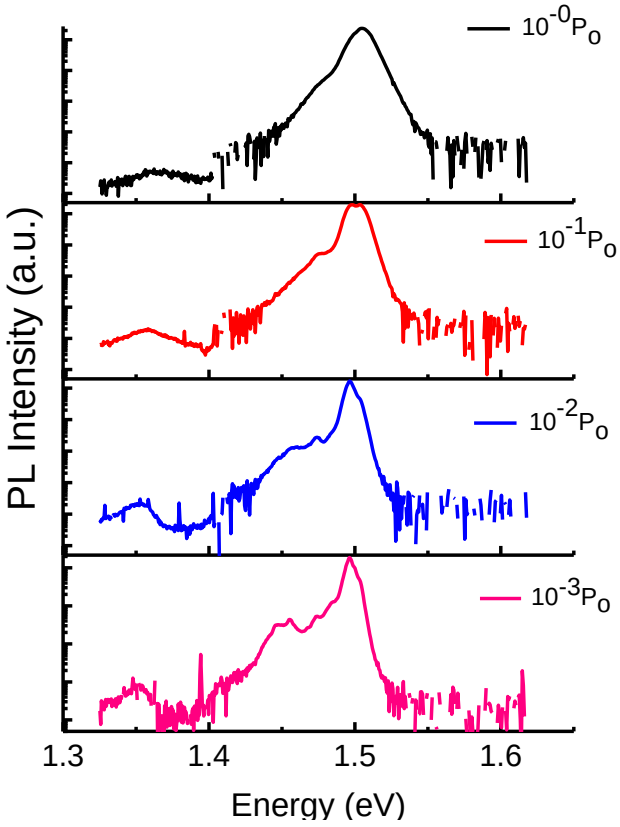

Figure 4.5: Logarithmic plot of *PL spectra of single nanowire (Ref8_NW1) at different excitation intensities. PL measurements for same excitation intensity are obtained for different integration times and stitched together, to obtain enough signal for low luminescing impurities without saturating the signal from main peaks. The data is normalized for different integration time before stitching.*

While conducting the reference PL measurements on as grown core-shell NWs, a small luminescence signal was unexpectedly observed at ~1.35 eV (Figure 4.5). Although the signal could be ~2000 times weaker as compared to the highest peak in the spectra, it was of interest for us because in literature this peak has been invariably reported to a transition involving copper acceptor states [12]. Copper contamination in GaAs, grown at high temperatures, is often reported in the previous photoluminescence studies of epitaxially grown planar GaAs [12]. But to the best of our knowledge, it has not been discussed in the NW photoluminescence studies so far. Copper has a high diffusion constant of $D = 1.1 \times 10^{-5}$ cm^2s^{-1} and solubility of 2×10^{16} cm^{-3} at 500°C, which is close the GaAs nanowire growth temperatures. Even in studies of high quality GaAs wafers, it was commonly reported as an unavoidable impurity[13][14], which supports the possibility of trace amounts of chemical impurities of copper atoms in our NW samples.

Further investigation of more individual NWs was carried out to statistically determine the probability of detecting luminescence at 1.35 eV. It was found that the luminescence is only distinguishable from the background when the signal is acquired for sufficiently long integration times at higher excitation intensities. Since the NWs under investigation had a very high PL efficiency, long integration times often saturate the camera for pixels corresponding to the high intensity peaks. Such a nonlinear condition is prohibited,to avoid saturation effects in the camera, which makes it easy to miss weak luminescence at ~1.35 eV. My observation for the next 18 NWs confirmed the presence of this luminescence for every individual NW. To rule out the possibility of stray luminescence, the results were reproduced with a 850 nm high pass filter, which blocks the signal from strong luminescing peak in the spectra, from entering the spectrometer. Different laser filters, optical fibers, gratings were also tried to rule out any unknown artifacts from the optics components.

To exclude contamination in a particular batch of NW due to impurities in the growth chamber, we looked into two more sets of data. Sample E1150713C and E1150810C were grown under similar conditions as the previously discussed sample E1150119C, but at different times, in the same growth chamber. Samples KY21 and IW20 were grown in different growth chambers but with similar recipes. All the samples exhibit equally high PL efficiency. For all these samples also, presence of copper related luminescence in the first 3 NWs was confirmed (Figure 4.6).

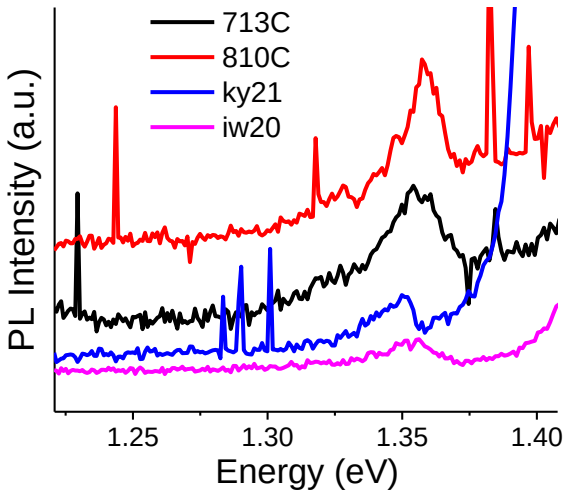

Figure 4.6: *PL spectrum of samples grown in different chambers and at different times, confirming the presence of copper related luminescence in all the available samples.*

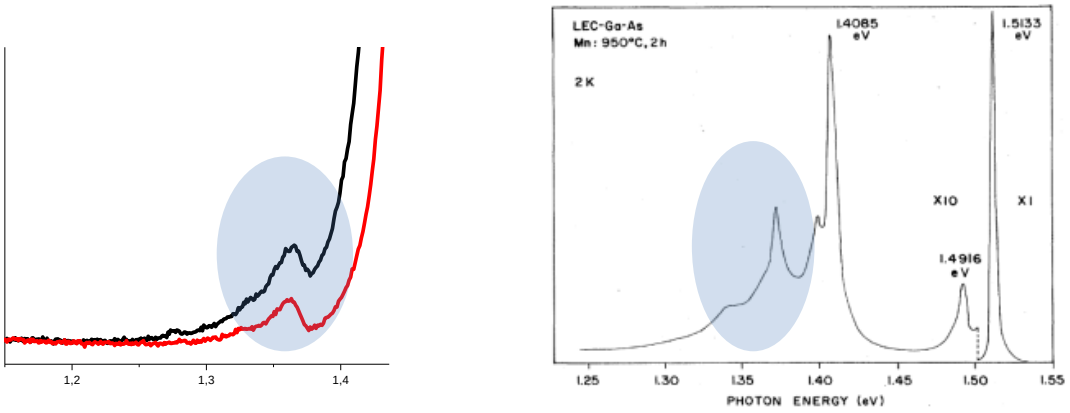

Figure 4.7 *Qualitative comparison of the asymmetry in* ***(a)*** *our PL signal with* ***(b)*** *the reported PL spectrum in literature*[12].

Figure 4.7 above highlights the asymmetric nature of the peak in our NWs, which could be similar to the LO phonon replicas of copper peak in bulk GaAs[12].Our results show strong similarities with the luminescence of copper in GaAs reported previously. Therefore, at this stage it was concluded that the possibility of copper contamination in our sample is very high.

PL study of 3 different epitaxially grown, high quality GaAs planar samples was also conducted to investigate the presence of copper and compare the luminescence of high quality GaAs NWs and planar samples. Nanowires are grown from gold seed particles which are evaporated and patterned on the substrate using lithography. The luminescence at ~1.35eV is persistent and present in the planar samples as well. This rules out the possibility of defect incorporation during gold patterning, done prior to NW growth.

All the three different wafer samples show the highest intensity peak at 1.513 eV, which is expected to originate from donor bound excitons. Another peak is observed at 1.491 eV, which is due to free to bound transitions of electrons in conduction band and holes in the shallow acceptors, due to carbon impurities. At low excitation intensity, free to bound recombination resulting in that peak at lower energy dominates the bound exciton transition, as expected.

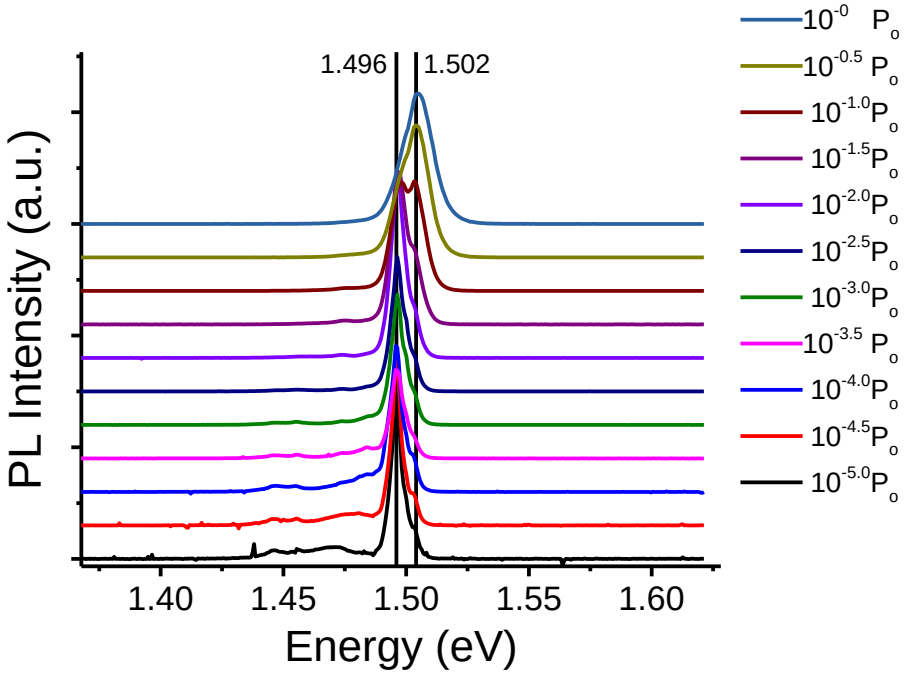

Figure 4.8: *Intensity dependent PL spectra for single nanowire (ref8_NW1), taken from sample E1150119C.*

Figure 4.8 shows typical excitation intensity dependent PL spectra of a representative NW, out of 33 measured, for the sample E1150119C. The plots are normalized to compensate for the different integration time and excitation intensity for each spectrum. We observe different interesting features in three different energy bands of the spectrum. First of them is the lowest energy band, centered on 1.35eV (Figure 4.7a), which is related to the copper acceptor states.

The second band is from 1.440 eV to 1.487 eV (Figure 4.8), which consists of peaks with a weak luminescence signal. It can be observed clearly in figure 4.8 that at high excitation intensities, the luminescence from this band merges with the rising edge of the most intense PL peak observed in our spectrum. At medium excitation intensities they are resolved in clearly identifiable sharp peaks and again appears as a broad luminescence at lower excitation intensities. Figure 4.8 shows the PL spectrum of 8 different NWs at a medium excitation intensity. Fine features appear to be consistently present in the NWs, but their relative intensities are not the same. Figure 4.9 compares the normalized intensity of different identified peak positions in our spectrum. The peaks for this energy band (1.445-1.48 eV) seem to saturate at high excitation.

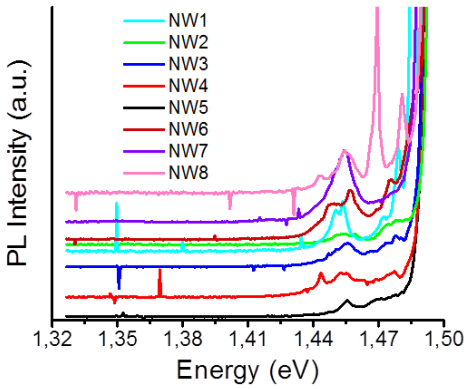

Figure 4.9: *PL spectrum of 8 different NWs taken NWs, from sample E1150119C, at medium excitation. intensity.*

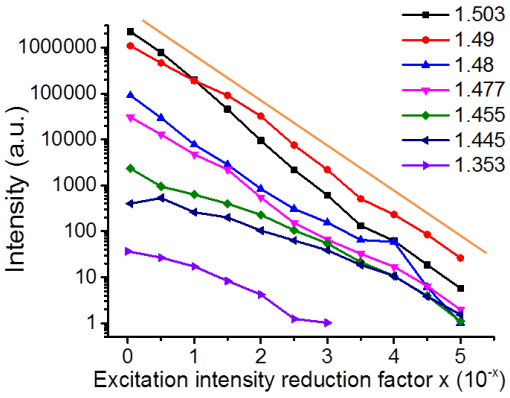

Figure 4.10: *Variation of different peaks in the PL spectra of a single NW(Ref8_Nw1) at different excitation intensities.*

The third band is the highest energy band which shows the highest intensity peak at 1.503 eV at high excitation intensities. As the excitation intensity is reduced, a peak at 1.496 eV resolves from the main peak and eventually dominates the luminescence signal for lower excitation intensities. For medium excitation, different closely spaced peaks appear as shoulder on the rising and falling edge of the peak at 1.496 eV. Figure 4.11 confirms that similar features are present in all the different nanowires in this sample.

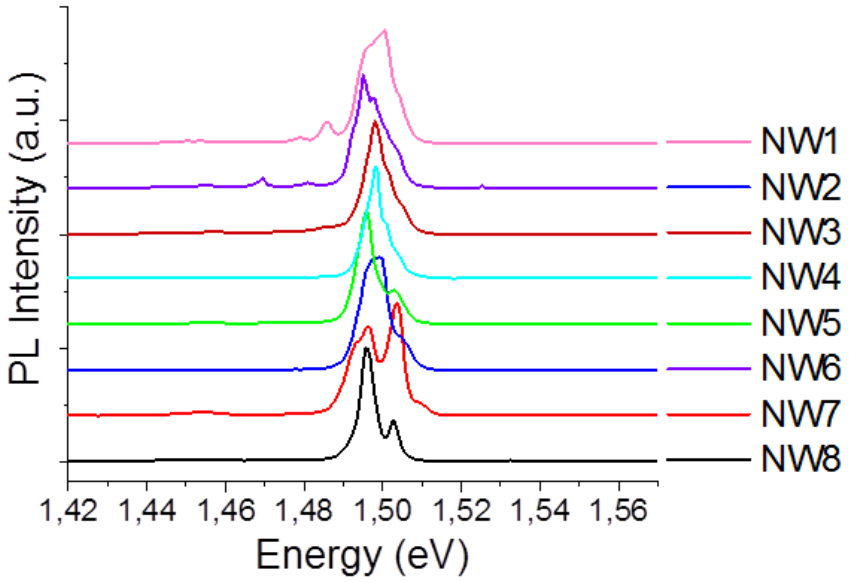

Figure 4.11: *PL spectrum of 8 different NWs, taken from sample E1150119C, at a medium excitation intensity. An offset is added to each spectrum for representation.*

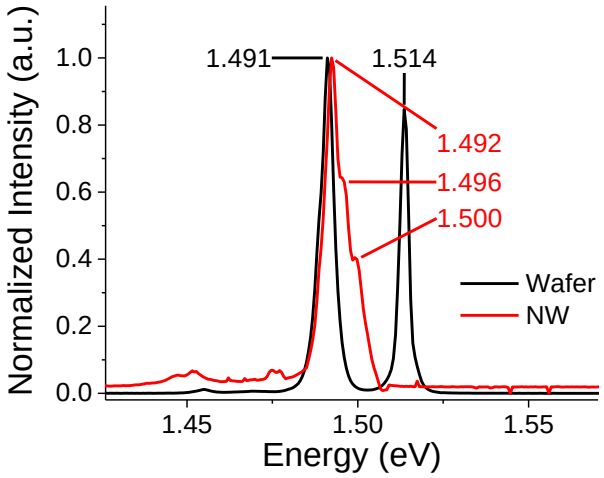

Figure 4.12: *Comparison of the PL luminescence from planar GaAs and GaAs/AlGaAs core shell nanowire. Both the spectrum are normalized to 0-1 scale for comparison purposes.*

Compared to the luminescence of donor bound exciton transitions in planar ZB GaAs, as shown in fig 4.12, the highest peak position of the NWs is shifted by ~10 meV towards lower energies. Comparing the luminescence of the NW and the wafer at lower excitation intensities, we see that the free to bound transitions, due to shallow carbon acceptors, at 1.491 eV are identical, except for the shoulder peaks around 1.499 eV. 1.502 eV is typically a bound acceptor exciton energy level in GaAs and a luminescence at this energy can result from $Cu_{Ga}V_{As}$ exciton bound to copper acceptors. Similarly a copper complex, $Cu_{Ga}V_{As}Cu_{Ga}$, bound to acceptor exciton can be responsible for luminescence at 1.48 eV as well[15].

A possible explanation for the most apparent difference in GaAs luminescence in planar and NWs, namely the absence of the donor bound exciton transition could be related to absence of donor bound impurities in our sample and giant oscillation strength for strong acceptor bound exciton transition in the NW. This is fairly justified because carbon and copper, both expected to be present in our sample are acceptor impurities. There is no evidence of donors being present in our sample. This is possible due to high quality and extremely controlled growth of these nanowires.

Also, we do not see free exciton transitions in our NW sample, the reason for this is thought to be the temperature of the wafer inside the cryostat. The temperature inside the cryostat is measured as 4 K at the cold finger. Temperature of the Si wafer is effectively higher than this and depends on the thermal conductivity of the silver glue. Further on the nanowires,

which are placed on the Si substrate, should have an even higher temperature. This would quench the free excitons which have a very small binding energy of ~5 meV, in GaAs.

4.2.2 Effect of diffusion or annealing on the PL spectrum

The available literature on the effect of annealing on the nanowires is not adequate. Also not much is known about diffusing copper at low temperatures. Based on the available information, copper diffusion was carried out at temperatures above 800 ^{o}C, but that is much higher than the growth temperature of GaAs nanowires, typically around 550 ^{o}C. Higher temperatures would mean a higher copper vapor pressure in the ampoule, which would favor copper diffusion. Therefore we started by annealing our samples at 550 ^{o}C followed by several experiments, as discussed in section 4.2.3, to successfully optimize the diffusion process.

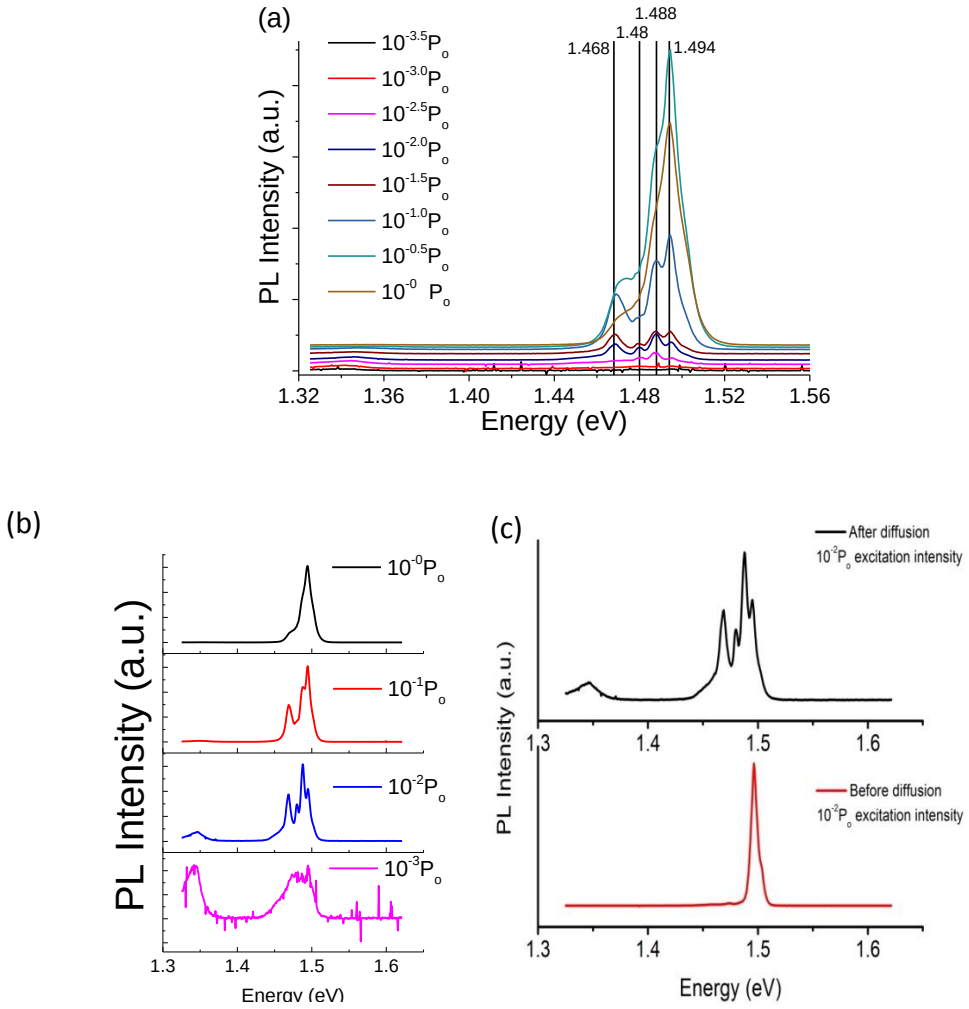

Figure 4.13: a) & **b)** *Intensity dependent PL spectra of the nanowire Ref8_NW1 after copper diffusion, at 450^{o}C for 2 hours, a fixed offset is added in the graphical representation for easier comparison* ***c)*** *comparison of PL spectra at medium excitation intensities before and after diffusion (normalized to 0-1 scale) for comparison.*

Figure 4.13a gives the Intensity dependent PL results of the same single nanowire (ref8_NW1) as discussed above, after diffusing copper at 450 ^{o}C for 2 hours. By comparing the PL spectrum at different excitation intensities, in figure 4.13b, we observe that the signal at ~1.35 eV has increased considerably after diffusion (Figure 4.13c). At 10^{-3} times the highest excitation intensity, the peak at 1.35 eV dominates the spectrum (Figure 4.13b). Even at higher excitation intensities it is comparable to other highest intensity peak in the spectra. This hints at the creation of additional copper states as a result of diffusion.

Besides the overall decrease in the PL efficiency, the relative intensities of the peaks has also changed after diffusion. At higher intensity a strong peak is seen at 1.494 eV and a small shoulder peak at 1.487 eV is observed with this peak. A broad luminescence peak at 1.46 eV merges with the rising edge of the peak at 1.494 eV. The PL efficiency increases super linearly with increase in the excitation intensity, evident by comparing figure 4.8 and figure 4.13. The broad luminescence at lower energies is better resolved in sharp luminescence peaks with luminescence at 1.487 eV becoming comparable to the brightest peak and the broad luminescence peak at 1.468 eV is well resolved and separated from the high energy luminescence. Upon further decrease in the excitation power, all the peaks intensities are comparable and the lower energy luminescence at 1.468 eV dominates the spectra. An extra peak at 1.48 eV is also resolved and is the weakest peak in the spectra.

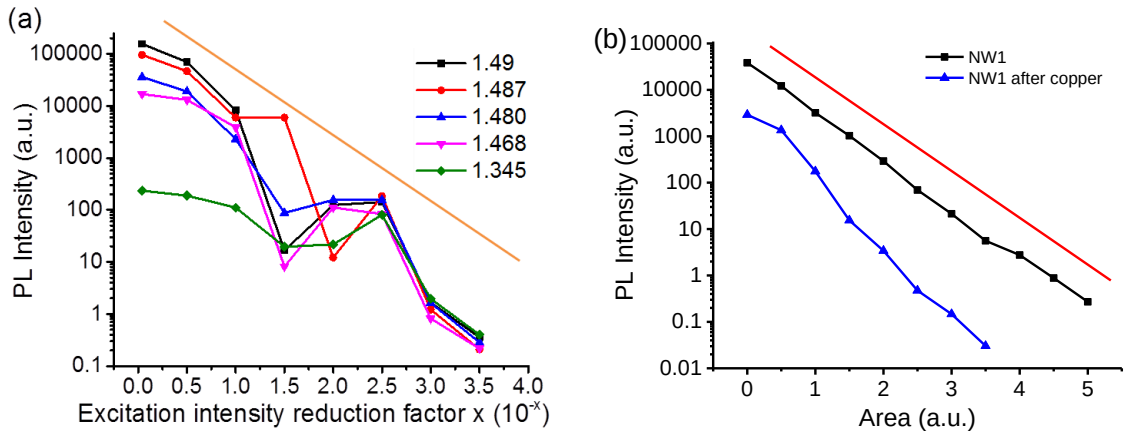

Figure 4.14: (a) *Variation of different peaks in the PL spectra of a single NW(Ref8_Nw1),after diffusion, at different excitation intensities.* **(b)** *Area under PL spectra for different excitation intensities for ref8_NW1 before and after copper diffusion where the straight line in the red gives the "linear" slope in the log-log curve.*

Figure 4.14a gives the evolution of different peak intensities with excitation intensity. The peaks in the spectrum show a super linear behavior with decrease in the intensities. In figure

4.14b the area under the PL spectra for different excitation intensities before and after diffusion are compared. Area under the graphs gives the total PL intensities of the spectrum. Before diffusion the total PL intensity changes linearly with the excitation intensity, but after diffusion the area under graph decreases super linearly with decreasing intensity. This hints at an increase in non-radiative defect states in this nanowire. Also by comparing the area under graph before and after diffusion, for a 30 times reduction of excitation intensity compared to the maximum power, we can estimate that the PL efficiency has decreased ~100 times. This gap widens for lower excitation intensities indicating optical degradation of our nanowires after annealing.

4.2.3 Optimization of diffusion

The optimization of the diffusion process involved a systematic study of the temperature variation to find the maximum temperature at which the copper diffusion can be carried out, without optical degradation. The amount of copper diffusion could then be manipulated by increasing or decreasing the duration.

Since we knew that GaAs nanowires are grown at 550 ^{o}C, we started by trying to diffuse copper in our wires at this temperature, for half an hour duration. The nanowires diffused at this temperature did not luminesce anymore, therefore we reduced the temperature while keeping the duration of the diffusion constant. We got some promising results for the nanowires diffused at 450 ^{o}C, for half an hour. The nanowires were luminescing very well even after the diffusion, but we could not see any increase in the copper signal. Therefore, we increased the diffusion duration to one hour. The luminescence results for this experiment are given in figure 4.15a.

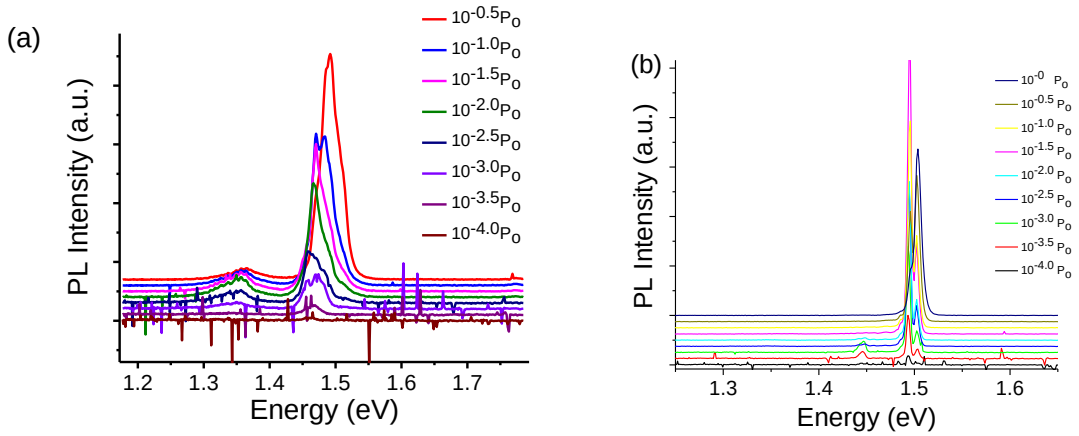

Figure 4.15: *PL spectra of a single nanowire after* **(a)** *copper diffusion and* **(b)** *annealing at 450°C for 1 hour.*

By comparing the integration time required to collect the same intensity counts at the highest excitation intensity, for many different wires before and after diffusion, I could see that the overall PL efficiency of the nanowires had reduced approximately 20 times. At higher excitation intensities the spectra is dominated by a broad luminescence at ~1.50 eV, with a shoulder peak on the high energy side at 1.510 eV. As the excitation intensity is reduced, it resolves into a double peak at 1.484 eV and 1.470 eV. For very low excitation intensities, the peak at 1.45 eV dominates the spectra. Luminescence signal at ~1.35 eV due to copper defects state seems to increase considerably after diffusion. The peak blue shifts with increasing excitation intensities. But it could not be concluded directly that the increase in luminescence signal is because of copper diffusion.

It could very well be possible that the increase in signal after annealing is only due to activation of the copper impurity atoms, already claimed to be present in the nanowire, rather than extra diffused copper atoms. Therefore, another experiment was performed in which the NWs were annealed at the same temperature and duration without the presence of copper. The PL spectrum for this sample, in figure 4.15b, does not reflect any increase in the copper signal. Instead even the background signal from the copper impurity atoms became extinct, maybe due to the degradation of the nanowires.

The results were promising and motivated us to create a setup, described in section 3.1, in which same NWs could be measured before and after annealing. This would help us to correlate the annealing effects better and also quantify the increase in the signal.

After arranging the setup, diffusion experiments were resumed, but surprisingly all our NWs annealed in the same conditions as before, did not luminesce after they had been annealed. Even for temperatures lower than 450^{o}C and shorter durations, the nanowires did not luminesce after annealing. We detected some leakage problem in our ampoule fabrication setup and the furnace also needed some recalibration.

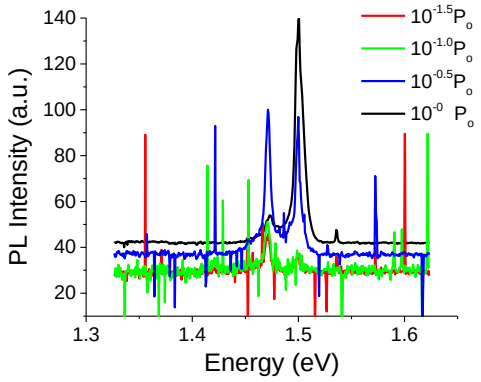

Figure 4.16: *PL spectra of a single nanowire after copper diffusion at 400^{o}C for 1 hour.*

Figure 4.16 gives the PL spectrum of a single nanowire annealed at 400^{o}C for one hour after solving the problems that had been discovered. The nanowires had optically degraded and we still faced some problems with reproducibility. It was reasoned that although we try to maintain the same pressure of 10^{-2} mbar, an unintentional pressure difference could affect the outgasing of As and create As vacancy defects in our NWs. To compensate for that, a small piece of GaAs was added to the ampoule with the sample. The GaAs piece would maintain the As overpressure in the ampoule and discourage out-gasing from the NWs. Preliminary measurements show that, indeed, the presence of GaAs in ampoule, during the annealing, reduces the degradation in the luminescence.

5 Conclusion and outlook

In this thesis, we attempted to do the first ever photoluminescence study of individual defects in semiconductors, in a way made possible by the nanowires. For this we aimed to diffuse copper in very low concentration in GaAs nanowires, and conduct PL studies on the diffused nanowires. While proceeding in this direction, it became clear that this cannot be accomplished with the available nanowire samples, as we detected copper contamination already in the undoped samples. I still continued working in this direction to create a foundation for continuation of this work in the future, when a suitable material becomes available.

We started by creating a highly efficient PL detection system which is the most crucial aspect of studies of single defects. The fact that we could detect even a weak signal from the unintentionally doped copper in our system, confirms the progress made in this direction. Additionally we established a reproducible method to measure the same nanowire, by using a computer controlled motorized stage.

Secondly, we conducted various experiments to find a suitable temperature to diffuse impurities in GaAs nanowires. We solved various challenges in this endeavor and finally we were able to confirm diffusion of copper in our samples without severe degradation of the nanowires. Further continuation of this work is required to make it more reproducible by understanding the effect of the different parameters involved in the diffusion.

Third, and the most interesting part was the PL study of the high quality GaAs material, in which the peak corresponding to the donor bound exciton is missing. Measurements on many different nanowires have confirmed the consistency of our results. Possible reasons for this could be the absence of donor bound exciton transitions in our sample or a shift in the position of the excitonic transitions. But this cannot be concluded with absolute certainty without performing a further study.

For future work on individual defect, it may be better to start again with a segment fully embedded in higher bandgap material, which would involve the combination of radial and axial heterostructures with a nanowire geometry. At this point it would be important to highlight that although it cannot be directly concluded from this thesis, the higher lattice mismatch between GaAs and GaP might be more difficult to optimize. The higher lattice mismatch can lead to distortion in the band structure of GaAs segments.

A possible solution to that would be to replace GaP with lattice matched AlGaAs. Although this would solve the problems with strain, a small GaAs segment surrounded by wide band gap material on all sides would experience more band bending effects. It would be exciting to pursue this further, and in the way find answers to all our concerns.

6 Acknowledgments

It gives me immense pleasure to thank my supervisor Dan Hessman. He was always around to answer my stupid questions and showed extreme patience in teaching me the intricacies of luminescence. I am extremely thankful to Lars Samuelson, who gave the idea of this project and throughout this thesis kept the charm of studying defects alive. A special thanks to Bo Monemar, the analysis of my results have benefitted from his unfathomable expertise in GaAs. I, thank the growers at SOL, Erik and Ingvar for taking special interest in this project and facilitating it. Thanks a lot Alexander for providing the starting point of this thesis, by growing nanowires for me.

I would like to thank Mariuscz and Sören, without your help in the labs this thesis could not have materialized. Also I would like to thank Niklas Sköld and Neimantas for being extremely cooperative in the PL lab. All those days when nothing seemed to work, my office mates were the best companions to hang around with. Thanks a lot for being there guys.

Annika, thank you for giving me a family away from home. Vishal, thankyou for being a very strong support system for me throughout this last year. Ali Hosseinnia, thankyou for pushing my limits with your constructive feedbacks. Eleni, you are one of the best things that happened to me in Lund. It's a really great feeling to have you guys as my friends.

In a special way, I would like to thank Dr. MK Roy, who motivated me to come this far in studying science.

In the end I would like to thank my family, your love is my strength.

7 References

1. Berg A. et al , *Nano Lett.*, **2016**, *16* (1), 656–662
2. Wallentin J. *SCIENCE* **2013** VOL 339
3. GILLEO M. A.; BAILEY P. T.; HILL D. E. *Phys. Rev.* **1968** 174
4. Rudolph D. et al *New. J. of Phys.* **2013** 15113032
5. Rashba, E. I.; Gurgenishvili, G. E *Sov. Phys. - Solid State*. **1962** 759–760.
6. Sturge M. D. *Phys. Rev.* **1963** 129, 2835
7. Sharma R. R. and Rodriguez S. *Phys. Rev.* **1967** 153, 823
8. Sharma R. R. and Rodriguez S. *Phys. Rev.* **1967** 159, 649
9. Boland J. L. et al *ACS Nano* **2016**, 10, 4219−4227
10. Vainorius N. et al. *Phys. Rev. B* **2014** 89, 165423
11. Aberg I. et al. *IEEE JOURNAL OF PHOTOVOLTAICS*, **2016** VOL. 6
12. Monemar B., Gislason H. P., and Wang Z. G. **1985** *Phys. Rev. B* 31, 7919,
13. Hall R.N. and Racette J.H., J. *Appl. Phys.* **1964** 35 379
14. F.C. Frank and D. Turnball, *Phys. Rev.* **1956** 104 617
15. Willman F.; Bimberg D.; Blätte M.; Phys. Rev. B **1973** 2473

Appendix A

Sample	Shell	GaP segment 1	GaAs	GaP segment 2	HCl
10394	-	10 min	5 min	5 min	0.4
10395	-	10 min	5 min	5 min	0.6
10396	AlGaAs 5sec	10 min	5 min	5 min	0.6
10397	AlGaAs 5sec	10 min	5 min	5 min	0.8
10450	AlGaAs 5sec GaAs secs	10 min	5 min	5 min	1
10451	AlGaAs 10sec GaAs secs	10 min	5 min	5 min	1
10452	GaInP 5 secs	10 min	5 min	5 min	1
10453	AlGaAs 5sec GaAs secs	10 min	5 min	5 min	1.2
10454	AlGaAs 5sec GaAs secs	10 min	2 min	5 min	1